balance of forces: even the presence of a few cross-linking points, with different solubility parameters, or of a few labeling units on the mobile chain may upset the compatibility.

(2) If we do have enough compatibility, we should be able to swell the dry gel in a reasonable time if the gel particles are small enough (below our micron). One of the interesting tricks used by the Mainz group[7] is based on the self-cross-linking of dilute PS chains: this generates very small gel particles—in fact a little too small, because the size of the particle may now become comparable to other lengths of interest.

(3) If the resulting gel is of acceptable optical quality, we can measure the diffusion coefficient D^* by the current optical techniques (with a small fraction of M chains labeled). D_{coop} is more difficult to reach, since in our swollen gels labeling all the mobile chains would probably lead to exceedingly high concentrations of labels. Also all measurements of D_{coop} (or of K) may be sensitive to defects in the gel texture (cracks or gel-free regions allowing for fast permeation).

(4) But, if all these difficulties can be ultimately removed, the transport properties will be extremely interesting. Figure 2 displays the amazing variety of regions that are expected. Some of these are very tentative. Some may be constantly unobservable (e.g., the thin region of tube renewal at $X < N_e$). But the broad features should remain relevant: for instance, the strangulation regime or the entangled regime M/M—where permeation becomes independent of the level of cross-linking!

Acknowledgment. The stimulus to write this paper was provided by Dr. H. Sillescu—in spite of the fact that our theoretical thoughts do not cover exactly his experimental conditions. Discussions with him, and with J. Klein, on related subjects, are gratefully acknowledged.

References and Notes

(1) Bastide, J.; Candau, S.; Leibler, L. *Macromolecules* **1981**, *14*, 719. See also ref 3 below.
(2) Brochard, F. *J. Phys.* (*Les Ulis, Fr.*) **1981**, *42*, 505.
(3) The most recent discussion of these notions is: Bastide, J. Ph.D. Thesis, University of Strasbourg, Strasbourg, 1985.
(4) Munch, J. P.; Candau, S.; Hild, G.; Herz, J. *J. Phys.* (*Les Ulis, Fr.*) **1977**, *38*, 971.
(5) de Gennes, P.-G. *Scaling Concepts in Polymer Physics*, 2nd ed.; Cornell University: Ithaca, NY, 1985, Chapter II.
(6) See for instance: Dullien, F. *Porous Media*; Academic: New York, 1979.
(7) Antonietti, M.; Sillescu, H. *Macromolecules* **1985**, *18*, 1162.
(8) Daoud, M.; de Gennes, P.-G. *J. Polym. Sci., Polym. Phys. Ed.* **1979**, *17*, 1971.
(9) Klein, J. *Macromolecules* **1978**, *11*, 852, and to be published.
(10) Monfort, J. P. Thèse, Université de Pau, 1984.
(11) Reference 5, Chapter VIII.
(12) Debye, P.; Bueche, A. M. *J. Chem. Phys.* **1948**, *16*, 573.
(13) Freed, K.; Edwards, S. F. *J. Chem. Phys.* **1974**, *61*, 3626.
(14) de Gennes, P.-G. *Macromolecules* **1976**, *9*, 594.
(15) Most of the existing data are in the range $N_e \ll X, M \ll N_e^2$. Thus in spite of the small area displayed in Figure 1, the regime of tube renewal is important in practice: see for instance Green, P.; Mills, P.; Palmström, C.; Mayer, J.; Kramer, E. *Phys. Rev. Lett.* **1984**, *53*, 2145.

Studies of Fiber Formation in Tubular Flow: Polypropylene and Poly(ethylene oxide)

A. J. McHugh* and R. H. Blunk†

Department of Chemical Engineering, University of Illinois, Urbana, Illinois 61801.
Received November 14, 1985

ABSTRACT: The flow-induced crystallization of isotactic polypropylene (PP) and poly(ethylene oxide) (PEO) solutions has been studied by using the technique of seeded growth in tubular flow. Similar to earlier studies with polyethylene, fiber formation from 0.01 wt % solutions in tetralin of an ultrahigh molecular weight polypropylene was found to occur by a sequence involving rapid formation of an unoriented, amorphous precursor followed by nucleation and axial growth of oriented crystallites in the precursor phase. Time constants for the development of birefringence in the precursor followed a pattern with temperature and solution flow rate similar to that of the earlier study and could be explained on the basis of stress-induced crystallization. Studies with 1 wt % solutions of a lower molecular weight polymer showed that the same precursor-to-crystalline fiber transformation occurs. Reduced initiation rates also enabled direct observations to be made of the precursor axial growth process. Fiber formation from solutions of an ultrahigh molecular weight PEO was found to be much reduced compared to that of either of the polypropylenes and was confined to a small temperature range slightly above the quiescent crystallization temperature. Observations were also made regarding entanglement formation during solution preparation. The discussion emphasizes the role of entanglement formation and chain stiffness on the precursor formation and fiber crystallization processes.

Introduction

The phenomenon of oriented fibrous crystallization during flow of high molecular weight polymer solutions has been extensively studied over the past two decades. Most investigations have employed Couette geometries, with a number of the more recent studies utilizing the surface growth technique. The latter experiments have contributed important information regarding the existence and probable nature of the entangled, gel-like liquid layer which forms on the rotor surface and from which fiber growth proceeds. Unfortunately, the existence of the self-regulating mechanism during surface growth and the possibility of postcrystallization drawing during fiber takeup severely limit the usefulness of the rate data one so obtains.[1]

A great deal of attention has also been directed to a number of methods for producing ultrahigh-modulus and -strength polyethylene fibers using techniques that are

*Author to whom correspondence should be addressed.
†Present address: General Motors Technical Center, Warren, MI 48090.

0024-9297/86/2219-1249$01.50/0

basically variations on flow-induced crystallization.[2] Although much has been learned from these studies regarding the details of fiber structure and properties, relatively few data have been generated that could be used to model basic mechanisms of the flow-induced phase transformation and structure formation processes.

For these reasons we have been directing our efforts to the technique that employs seeded growth in a free-flow geometry since it offers a much better means for directly studying the phenomenon of flow-induced crystallization. In recent papers[3-5] we reported a number of new findings concerning the flow-induced crystallization behavior of ultrahigh molecular weight polyethylene (UHMWPE) solutions in a tubular flow geometry. Direct observation under polarized light illumination showed that the fibrillar transformation process always initiates by the formation of a concentrated, amorphous precursor that is optically isotropic. With continued flow one sees a gradual development of birefringence due to centers of oriented crystallization which nucleate randomly along the precursor axis, eventually merging to form a fully birefringent, oriented, crystalline fiber. The timed sequence of events for precursor formation, crystal nucleation, and completion of birefringence shows a marked dependence on the solution flow rate and crystallization temperature.[4] An interpretation of crystal nucleation times was given in terms of stress-induced nucleation theory in which the precursor phase was modeled as a network structure containing a high density of trapped entanglements which act as effective cross-links transmitting stress from the streaming solution.[5]

Among other things, these results offer clear evidence that the phenomenon of flow-induced crystallization and that of flow-induced structure formation, often observed in rheological studies, are highly interrelated. One also has the suggestion that since a necessary condition for crystallization is the occurrence of precursor formation, the molecular weight fractionation, previously associated with crystallization, may best be modeled as a type of liquid–liquid phase separation.[6,7]

We have been further studying the flow-induced crystallization behavior of several high molecular weight polymer/solvent systems with our tubular flow apparatus. Our objectives have been to investigate the universality of the precursor-oriented crystallization sequence and to develop a broader data base for the analysis of time constants associated respectively with precursor formation, crystal nucleation, and final fiber crystallization. The purpose of this paper is to present and discuss the results of our recently completed studies on polypropylene and poly(ethylene oxide) solutions. These results show that ultrahigh molecular weight polypropylene undergoes a transformation process under flow very similar to that of polyethylene. Experiments with a lower molecular weight polymer and a high molecular weight poly(ethylene oxide) have also led to a number of further insights regarding the nature of the precursor axial growth and fiber crystallization processes.

Experimental Section

Materials. The majority of the fiber growth experiments were carried out with an ultrahigh molecular weight polypropylene (UHMWPP), supplied by Himont, having an intrinsic viscosity of 19.4 dL/g in decalin, which corresponds to an average molecular weight of about 3×10^6. On the basis of a decalin solubles test, the fraction of atactic material has been estimated to be 1.5%.[8] Polymer concentration was 0.01 wt % in reagent grade tetralin to which 0.25 wt % of the antioxidant 3-*tert*-butyl-4-hydroxy-5-methylphenyl sulfide (Santanox) was added. Additional crystallization runs were also made with various concentration solutions, in tetralin, of a lower molecular weight polypropylene (LMWPP), supplied by Shell (homopolymer grade 5520), having a melt index of 4.8 and an intrinsic viscosity of 4 dL/g. The ultrahigh molecular weight poly(ethylene oxide) (UHMWPEO) (Aldrich Chemical Co.) that was used had an average molecular weight of 4×10^6 and was dissolved to various concentrations in absolute ethanol.

Solution Preparation. Since the question of stirring history effects (during solution) on the phase separation behavior of ultrahigh molecular weight solutions is of critical importance, a series of qualitative experiments was carried out to evaluate the earlier used solutions procedure and to establish a basis for the present study. Several comments will be made here as they bear on our interpretation of the precursor formation process. We have also been carrying out extensive quantitative studies of the viscosity and shear-thickening behavior of these solutions,[9] the details of which will be the subject of future publications.

We have found that the viscosity behavior and elasticity of 0.01 wt % solutions of our UHMWPE and UHMWPP in their respective solvents are qualitatively and quantitatively similar. For example at 110 °C the zero-shear viscosities are about 0.5 and 0.7 cP, respectively, and both solutions exhibited a noticeable Weissenburg or rod-climbing effect on gentle stirring, indicating the occurrence of entanglement network formation.[10] Upon slow cooling either solution to 80 °C, in the quiescent state, immediately following preparation, phase-separated gelatinous structures formed. However, when the solutions were held at their respective preparation temperatures (130 and 170 °C) for approximately 0.5–1 h after dissolving and then cooled, single-crystal aggregates always formed. The latter standing times had been used in the previous study[4] and were also followed in the present experiments to eliminate memory effects associated with stirring and ensure that liquid structure formation occurred during flow at the selected crystallization temperature and not at the solution preparation temperature.

The lower molecular weight polypropylene (LMWPP) solutions did not display a discernible Weissenburg effect until concentrations on the order of 1 wt % and these solutions also exhibited a much lesser degree of gel-like phase separation upon cooling. The 0.1 wt % UHMWPEO/ethanol solutions that were investigated were prepared by slowly sprinkling the resin into gently stirred ethanol at 60 °C. Since severe degradation of PEO solutions is known to occur at moderate shear rates,[11] a reference solution was also prepared under a nitrogen atmosphere. On cooling to 40 °C neither phase separation nor any observable Weissenburg effect occurred. Slow cooling to 31 °C without stirring led to complete precipitation (~1 day) of the dissolved polymer as single-crystal aggregates, further indicating the lack of any significant network formation.

Apparatus and Procedures. The fiber formation process was studied by streaming solution past a stationary seed anchored near the entrance of a 2-mm-i.d. capillary tube. Growth from the seed surface was monitored by observing the process under polarized light with simultaneous video recording. With the exception of several minor design changes needed to extend the working temperature to 170 °C for the polypropylene solutions,[12] the flow loop and apparatus, optics, video recording, and solution preparation techniques were the same as previously described.[4] Temperature and flow rate control was also maintained within the previous limits (±0.3 °C and ±10%). Unlike UHMWPE, flexible filaments did not function well as seed materials for the UHMWPP solutions. Consistent with earlier studies[13] we have found that polypropylene solutions must be significantly undercooled (more so that PE) in order to achieve reasonable rates of crystallization. Below 104 °C, the UHMWPP readily phase separated under flow, coating the seed with a thick, liquid layer, causing excessive shrinkage, poor adhesion, and highly nonuniform precursor formation. Above 104 °C, lessened layer formation led to strong attachment of fine, unform precursors, and, under these conditions, the process resembled that seen with the UHMWPE. However, at these higher temperatures, crystal transformation times exceeded those possible by complete drainage of the 4-L solution reservoir.

A thin stainless steel wire (600-μm diameter) with small indentations on its tip was found to give adequate surface attachment and uniform precursor development over a convenient range

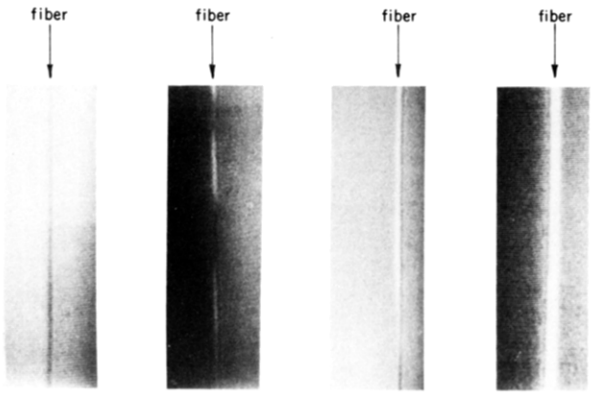

Figure 1. Precursor-to-crystalline transformation process at 90 °C and a solution flow rate of 2500 cm/min. Sequence from left viewed through crossed polars at fixed position in flow tube. Time interval between photos is 25 s with the exception of the final photo, which was taken 3 min after the one preceding it.

of temperatures below 104 °C with the UHMWPP. During initial flow periods, several precursor adsorption–breakage cycles were often observed before adequate seed attachment was achieved; thus reliable values of precursor initiation time could not be obtained with these seeds. (Attempts were made to enhance precursor/seed attachment by using optical glass fibers and a Teflon/ethylene copolymer coated wire, without noticeable improvement.) All runs with the UHMWPP to be described were therefore made with the wire seed, which was positioned and centered in the flow tube using the previously described holder.[4]

In the case of the LMWPP a number of runs were carried out with a 1 wt % solution in tetralin. Fiber formation, as expected, was much less in magnitude than with the UHMWPP, allowing the use of a thin polypropylene seed filament. The latter was prepared by spinning a molten filament from a 0.1-mm-diameter capillary die followed by rapid hot drawing to produce a fiber diameter of approximately 50 μm. Details regarding the fiber growth experiments with the UHMWPEO/ethanol system will be discussed later.

Total birefringence and melting point data were obtained for a representative group of fibers grown from the UHMWPP solutions at various flow rates and temperatures. Several of these fibers were also analyzed by X-ray diffraction and electron microscopy. In all cases the techniques used for sample preparation and optical analysis were the same as those described previously.[4]

General Observations

(i) UHMWPP Fiber Growth. The general fiber formation pattern with the UHMWPP solutions was essentially the same as that found earlier with the UHMWPE, except for the crystallization temperature range and characteristic transformation times, which differed considerably. Figure 1 is a series of still photos illustrating a typical precursor-to-crystalline fiber transformation sequence as viewed through crossed polars 3 cm downstream from the seed tip. The average flow velocity, $\langle v \rangle$, and crystallization temperature, T_x, in this case were 2500 cm/min and 90 °C, respectively. The sequence shown left to right was shot at 25-s intervals after flow commenced, with the exception of the final photo, which was taken after a 3-min interval following development of the uniformly birefringent state shown in the third photo. The optically isotropic precursor fiber shown on the far left formed almost immediately with the onset of flow and extended the entire 20-cm length of the flow tube. Under most conditions such precursors rapidly thickened to a finite diameter (typically 10–25 μm) before crystallizing axially as shown in the second and third photos. Rotation of the polars in the crossed configuration produced no change in the lack of light transmittance of the precursors while the 45° isocline pattern characteristic of uniaxially oriented

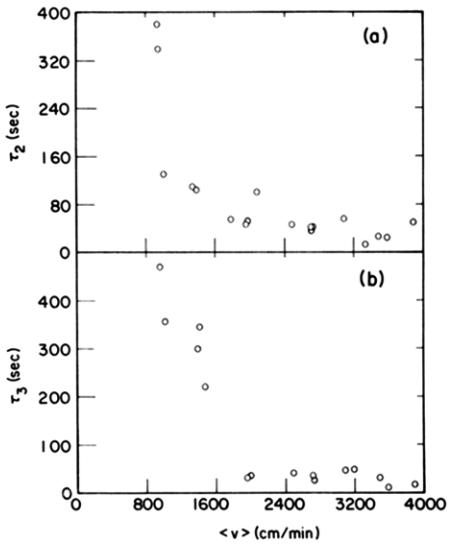

Figure 2. Induction times vs. flow velocity for various constant temperatures in the range 89–90 °C: (a) time τ_2 relative to precursor appearance for initiation of crystal birefringence; (b) time τ_3 relative to τ_2 for development of uniform birefringence.

crystallization was observed once the fibers became fully birefringent. Axial development of birefringence (second photo) is seen to occur by a pattern indicative of random nucleation of oriented crystallites, similar to that found with polyethylene.

The third photo in the sequence shows the state of birefringence in the fiber shortly after the growing centers have completely merged. In the case of polyethylene under free-flow conditions, fiber birefringence was found to remain essentially constant beyond such a point. However, the polypropylene fibers continued to show an increase in birefringence over a time period of several minutes, reaching a much higher final state of saturation as shown in the last photo of the sequence of Figure 1. For a given run, the timed sequence of these events was essentially the same regardless of axial position except for the region immediately downstream from the seed. As before,[4] the development of birefringence was found to be slowest at the seed, and, in the region immediately downstream, a strong taper could be seen from the seed diameter (600 μm) to the downstream fiber diameter (~25 μm). Such tapering behavior has been commented on elsewhere[14] and, we believe, simply represents an artifact of the seed size.

During the course of the axial growth of the birefringence centers, a periodic flashing pattern occurred similar in nature to that which was observed during polyethylene fiber transformation at higher temperatures and lower flow rates. In the present case, however, such flashing was observed at all flow rates studied over the temperature range 83–104 °C. Below 83 °C, crystal growth rate increased to the point that uniformly birefringent fibers formed almost immediately with flow while above 104 °C, as noted earlier, precursors did not crystallize over the time scales available for flow. However, precursor formation was observed at temperatures as high as 120 °C.

Time constants for the initiation and completion of axial birefringence development were obtained from slow-motion replay of the videotaped sequence for fiber segments viewed at a fixed position 3 cm downstream from the seed. Although reliable data could not be obtained for precursor intiation times, patterns with $\langle v \rangle$ and T_x, similar to those found with UHMWPE, were seen in the other two time constants and are shown in Figures 2 and 3. Figure 2a shows the induction time for initiation of crystalline birefringence (flashing), τ_2, relative to the time of stable

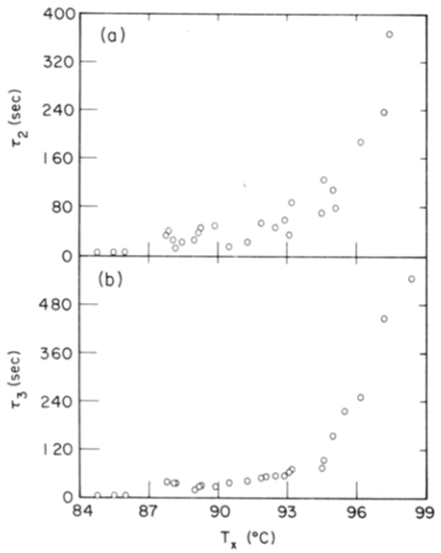

Figure 3. Induction times τ_2 (a) and τ_3 (b) vs. crystallization temperature. Data are for range of flow rates in plateau region shown in Figure 2.

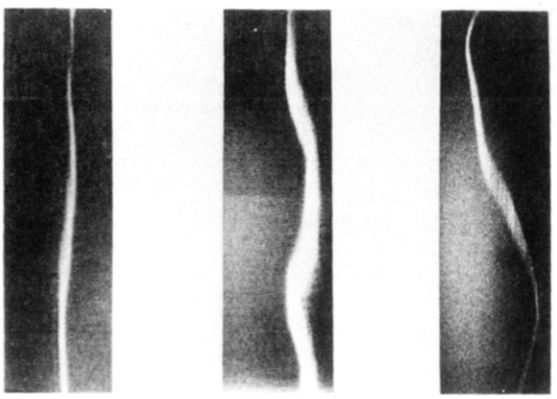

Figure 4. Sequence showing typical relaxation process in completely transformed polypropylene fibers on cessation of flow.

precursor formation, and Figure 2b shows the time, τ_3, relative to τ_2 for the development of uniform birefringence in the fiber. Each data point represents a fixed temperature; however, the data shown have been plotted for a range between 89 and 90 °C to more clearly show the trend of decreasing induction time with average flow velocity. One also sees that a plateau is reached in both time constants around $\langle v \rangle = \langle v \rangle_p \sim 2000$ cm/min. τ_2 and τ_3 rapidly increase from seconds to minutes below $\langle v \rangle_p$ and become essentially independent of $\langle v \rangle$ above it. Figure 3 shows the strong influence of crystallization temperature on the transformation times in the flow plateau region.

Postflow phenomena were similar to those seen with UHMWPE. Occasionally, the downstream end of a fiber became entangled in the flow tube stopcock, resulting in an additional increase in fiber birefringence. More frequently, however, with the cessation of flow, fibers would partially shrink (recoil), resulting in a slight decrease in fiber birefringence as shown in Figure 4. Such behavior was most pronounced at the higher temperatures and lower flow rates.

(ii) LMWPP and UHMWPEO Fiber Growth. Fiber growth from 1 wt % solutions of the lower molecular weight polypropylene displayed a considerably more random behavior, due largely to the much reduced tendency for precursor formation. However, in consequence of reduced precursor formation rates, observations of the axial growth process could be made by scanning the tube during

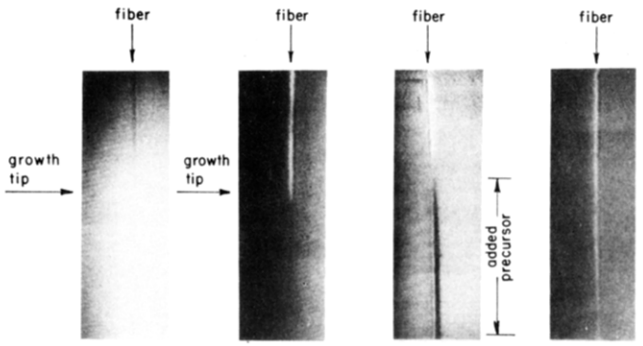

Figure 5. Precursor axial growth–crystalline transformation process as viewed at a fixed position in the flow tube. Sequence shown is for lower molecular weight polypropylene. See text for details.

flow, something that had not been possible with either of the UHMW polymers. The timed sequence for the LMWPP amorphous-to-crystalline transformation varied axially along the length of the precursor, with growth occurring in either of two fashions. In the range of flow rates from 1800 to 2100 cm/min and for crystallization temperatures between 88 and 90 °C, the eventual precursor-to-crystal transformation process was very similar to that of the UHMWPP once the precursor had grown the full length of the flow tube. However, axial growth of the precursor was quite random, generally starting with an approximately 1-cm length attaching to the seed filament shortly after flow. Such fibers were similar in appearance to that shown in the first photo of the sequence illustrated in Figure 5. Axial growth was found to proceed by a series of steps involving rapid attachment and detachment of short sections of amorphous material, with the entire process taking about 10 s before the precursor extended the length of the flow tube. After an additional induction period of approximately 20–25 s, centers of birefringence then nucleated at various axial positions in the precursor followed by longitudinal merging to form a fully birefringent fiber. The latter nucleation and growth events, though random, followed a sequential pattern at a given position quite similar to that shown in Figure 1 for the UHMW fiber.

At somewhat higher flow rates (~2500–3000 cm/min) and essentially the same or slightly lower temperatures, an alternate growth process occurred, a typical example of which is shown in sequence in Figure 5. In this case, the upstream segment of precursor is seem to transform to a completely birefringent fiber (second photo) before additional axial growth takes place (third photo) followed by transformation of the added segment. The combination of increased crystallization rate at the slightly lower temperature (87 °C) and decreased effectiveness of the chain entanglement process at the precursor tip at the higher flow rate (2900 cm/min) causes the precursor segment to first crystallize and then act as a seed for further attachment of a new segment. Relative to the near-instantaneous formation time of the initial segment, induction times were approximately 5, 25, and 30 s respectively for the processes of birefringence development in the precursor segment, attachment of the additional segment, and formation of the completely transformed fiber depicted in Figure 5.

Postflow phenomena for these fibers showed a similar behavior to that of the UHMW polymer in that completely transformed fibers coiled up with some loss of birefringence on cessation of flow. However, in this case drastic shrinkage occurred on extraction of the fibers from the crystallizing tube, which prohibited us from making any property characterizations. (The extracted LMWPP and

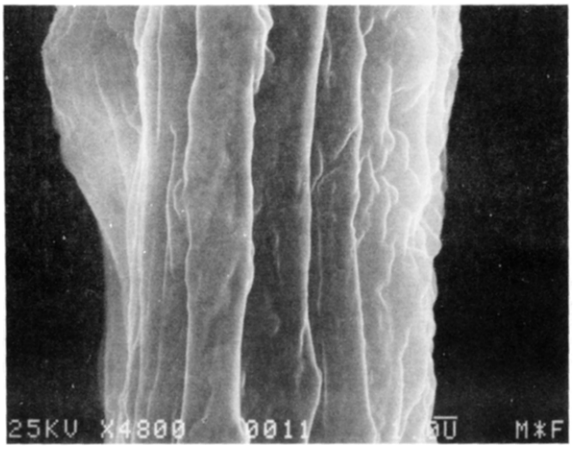

Figure 6. Scanning electron micrograph of high molecular weight polypropylene fiber grown at 93 °C and 2400 cm/min solution flow rate.

Table I
Optical/Hot-Stage Microscopy Measurements on Some Representative Isotactic Polypropylene Fibers[a]

T_x, °C	$\langle v \rangle$, cm/min	$\bar{\Delta}$	T_m', °C	T_m'', °C	T_m''', °C	T_m*, °C
97	1400	0.0027	159.4	164.7	173.3	163.1
94	1400	0.0054	163.1	165.0	172.9	162.9
88	1400	0.0099	161.3	163.7	175.9	162.9
88	2100	0.0110	162.7	163.9	178.6	164.1
97	1100	0.0024	164.1	168.7	172.1	167.8
97	3200	0.0035	161.5	166.3	173.5	168.8

[a] See text for explanation of symbols.

UHMWPP fibers shrank from 20 cm to about 0.5 and 12 cm in length, respectively.)

Finally, the fiber-forming characteristics of the PEO/ethanol system were studied for several solutions in the concentration range between 0.1 and 0.2 wt %. Runs were made over a range of temperatures (31–40 °C) and flow rates utilizing a flexible, polyethylene seed fiber. Consistent with the qualitative indications regarding the low elasticity of these solutions, mentioned earlier, we found that precursor formation and fiber growth were weak at best. For example between 35 and 37 °C and flow velocities below 2500 cm/min, short (~2 cm) and quite faint precursor segments were seen. Such precursors never extended the length of the flow tube and generally transformed within 5 s to complete birefringence. Above 37 °C no precursor formation occurred, while fibers obtained below 35 °C shrank to such an extent on extraction from the flow tube that they were not usuable for analysis.

(iii) Fiber Analysis. Figure 6 shows a scanning electron micrograph of an UHMWPP fiber that was grown at T_x = 93 °C and $\langle v \rangle$ = 2400 cm/min. The multifibrillar substructure is typical and similar in appearance to that observed with polyethylene fibers.[4,15] The excess solution that adhered to the fiber on extraction from the flow tube has formed a thin film on these fibrils, thereby obscuring striations normally associated with the shish kebob microstructure.

Trends in the overall birefringence and thermal behavior are illustrated in the data of Table I. Values for the room-temperature birefringence ($\bar{\Delta}$) are based on an average of five readings taken along a 2-cm length of fiber. One sees a trend here that is similar to that observed earlier with the polyethylene fibers in that overall birefringence is more affected by crystallization temperature than flow velocity. One also sees the same trend of an increase in birefringence occurring with either decreasing T_x at constant $\langle v \rangle$ or increasing $\langle v \rangle$ at constant T_x. Hence fibers grown under the combination of lower temperature and higher flow rate develop a higher degree of internal order.

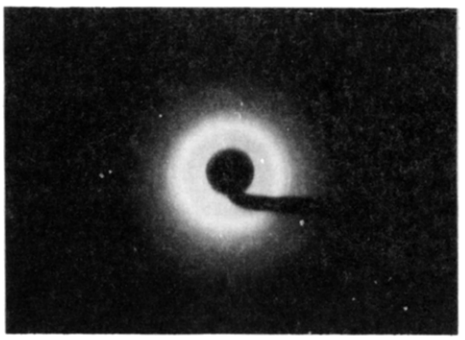

Figure 7. Flat-film X-ray diffraction pattern of polypropylene fiber grown at 88 °C and a solution flow rate in the plateau region.

The melting temperatures shown in Table I were obtained on 3-cm lengths of fiber that were coiled inside a drop of silicone oil, allowing them to freely contract on heating at the rate of 10 °C/min. The four temperatures listed are T_m', the onset of fiber melting as indicated by the start of fiber contraction; T_m'', the melting point corresponding to extensive fiber contraction; T_m''', the temperature at which final traces of birefringence disappear; and T_m*, the melting temperature after recrystallization. The qualitative trend displayed by these data is also quite similar to that of UHMPE. By comparison the melting point of thin, spherulitic films of the UHMWPP was found to be 162 °C.

An X-ray diffraction pattern for a fiber grown in the velocity plateau region at T_x = 88 °C is shown in Figure 7. The extraneous spots on the X-ray film are a result of both the long exposure times (3 days) required and the presence of the semioriented film which crystallized on the surface of the fiber on extraction from the flow tube. The equatorial diffraction arcs that can be seen are the (110), (040), and (130) reflections characteristic of *c*-axis orientation (although not apparent here, faint (111) reflections were also seen). Comparison with X-ray diffraction patterns and birefringence data in the literature[16] indicates that the overall orientation is equivalent to that of a fiber elongated about 100%.

An extensive discussion was given in our earlier paper[5] regarding the interpretation of birefringence initiation times in terms of stress-induced crystallization theory. Formal analysis of the crystal nucleation rate requires a knowledge of the effects of solvent concentration, entanglement concentration, and stress on the equilibrium melting temperature, T_m, for an infinite crystal in the stressed precursor phase. Fortunately, for the conditions of our experiment the applied stress due to flow is low enough that its effect can be neglected. Likewise, though the reduction in melting point as a function of solvent and entanglement density is not directly analyzable, the effect of these variables on T_m presumably reaches a constant in the velocity plateau region. Consequently approximating T_m with values in the vicinity of T_m° (the equilibrium melting point associated with the quiescent melt) leads to a reasonable linear fit of ln $(1/\tau_2)$ vs. $T_m/T_x(T_m - T_x)$, which is independent of flow rate for a range of velocities in the plateau region.[5] Figure 8 shows that a similar linear pattern results for the UHMWPP τ_2 data in the velocity plateau region. Since a wide range of uncertainty exists with regard to the properly extrapolated value of T_m for polypropylene,[17] the measured value of 162 °C obtained by hot stage has been used.

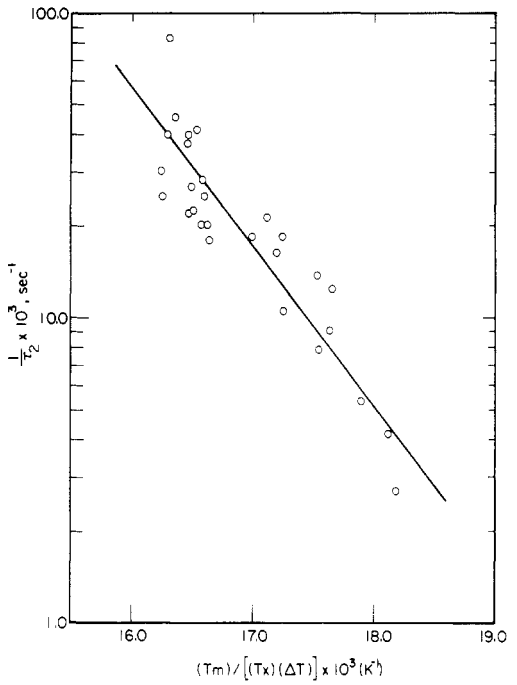

Figure 8. Plot of induction time, τ_2, against undercooling $(T_m/T_x(T_m - T_x))$ for various flow velocities in the plateau region.

Discussion

The results presented in this paper and our earlier study offer conclusive evidence that the sequence of precursor formation followed by oriented crystallization is the characteristic process by which flow-induced crystallization occurs under free-growth conditions. For a given system the relative time constants for the individual rates involved depend strongly on molecular weight, concentration, temperature, and flow rate (i.e., applied stress field). It is in fact a consequence of the relatively low stresses characteristic of the free-flow technique that one is able to clearly observe the transformation process in sequence. Under conditions of higher flow rate or lower undercooling, rates increase to the point that the sequence of precursor formation followed by crystal nucleation and axial growth is no longer distinguishable in the overall fiber formation process. At the other extreme, under conditions of low entanglement formation (i.e., combinations of lower molecular weight, concentration, and higher growth temperature) one finds either that very weak precursors and subsequent crystalline fibers result or that no transformation occurs at all. The arguments we presented earlier[4,5] for concluding that precursors are highly concentrated, amorphous phases hold equally well in the present case. We also feel that the good qualitative agreement between the plot shown in Figure 8 and the plots in Figure 1 of ref 5 offers further substantiation for the interpretation that crystal nucleation in the precursor phase can be treated on the basis of stress-induced crystallization theory. In both cases one is observing a lower bound behavior pattern in the sense that the applied stress is small and therefore only moderately perturbs the crystal nucleation process while still having a measurable effect on crystal orientation.

An understanding of the precise nature of the events leading up to precursor appearance is, of course, critical to the entire process. On the basis of several of the observations presented in this paper, as well as our ongoing studies, we feel that the development of a dense network of chain entanglements under flow followed by subsequent liquid phase separation is the most likely sequence of events by which precursors develop. We have been generating data that show that initiation of the chain entanglement process leads to a well-defined shear-thickening pattern in the reduced-viscosity behavior of our fiber-forming solutions.[9] These experiments are especially useful in that one is observing the phenomenon under flow conditions (i.e., shear rate and flow kinematics) similar to those characteristic of the tubular growth process.

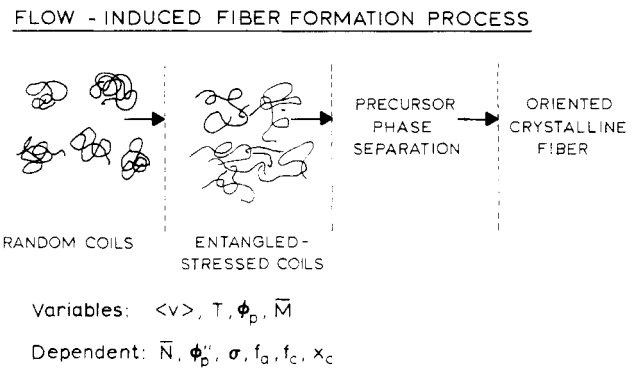

Figure 9. Sketch of coil-to-fiber flow-induced transformation process. Listed also are the primary independent and dependent variables.

Figure 9 shows a pictorial representation of the series of steps we believe to be involved in the flow-induced coil-to-crystalline fiber transformation process. Listed also are the primary process variables, which include the polymer concentration, ϕ_P, and molecular weight, $\bar{M}$, as well as solution flow rate and temperature. For given values of these quantities, the sequence from relaxed, random coil to entangled stressed coils will be set by kinetic processes during the flow history, leading ultimately through a thermodynamically driven phase separation, to the liquid precursor state. The flow entanglement process effectively fixes the number density of entanglement sites, $\bar{N}$, as well as the polymer concentration in the liquid precursor phase, ϕ_p''. This in turn will fix the effective stress, σ, which can be transmitted to the precursor from the streaming solution, and, in consequence of the arguments discussed earlier, the effective melting temperature and stress-induced crystallization behavior will be set. The final crystallized fiber will then be characterized by a given orientational state for both the crystalline, f_c, and amorphous, f_a, regions and a degree of crystallinity, x_c. The latter variables, once arrived at, fix essentially all of the important physical properties of the fiber. A detailed knowledge of both the entanglement-to-precursor formation process and the history of the oriented crystal growth process would enable one to construct a complete model for the overall process and, at least in principle, enable the calculation of fiber properties from a knowledge of the process variables. We are currently developing models of these processes based on our ongoing experiments and will present details of our studies in future publications.

For the present purposes the differences in behavior pattern between the PP and PEO solutions can also be rationalized on the basis of earlier studies showing that flow-induced crystallization behavior can be correlated with the inherent chain stiffness of a polymer.[11,18-20] Generally speaking, the range of temperatures over which fibrous crystallization occurs from stirred solutions, as well as the amount of extended-chain crystals in the fibers, are found to increase with the stiffness factor.[20] Superposed on this are, as mentioned, both the kinetic and thermodynamic aspects of the chain entanglement process which will further influence the effective chain stiffness under flow. In the latter case, we have shown elsewhere[6,7] that the appearance and stability of a concentrated, liquid

phase formation can be rationalized by treating the system of entangled, stressed chains under flow as equivalent to a thermodynamic model system consiting of chains with a reduced flexibility. In such a case, one finds that a liquid–liquid phase separation always occurs in a fashion such that chains in the more concentrated phase have a lower flexibility than those in the dilute phase. For the UHMWPP and UHMWPEO systems, the inherent chain stiffness factors are 1.61 and 1.38, respectively, which correlates with our observation of well-defined precursor formation in PP over a wide range of temperatures 83–120 °C) well in excess of the normal, quiescent crystallization temperature (~72 °C) while UHMWPEO precursors were only found over a narrow range 35–36 °C) near the PEO quiescent crystallization temperature (~31 °C). Likewise since the PP precursors are stable at small undercoolings, they have measurable lifetimes before the crystalline transformation occurs as opposed to the PEO precursors, which, since their effective undercooling is larger, transform almost immediately. On the basis of the poor integrity of the PEO fibers and observations from earlier DSC studies[20] one also expects little or no extended-chain crystals to be present in the fibers that do form. These results are also consistent with the strong tendency for stirring-induced network formation and subsequent phase separation we observed with the PP as opposed to the much greater tendency of the stirred PEO solutions to form crystal aggregates on cooling.

Clearly, molecular weight and concentration also play an important role in the precursor formation–crystallization process as noted by the fact that fibers did not form from 1 wt % LMWPP solutions above 105 °C nor from 0.1% solutions under any conditions. Furthermore, though crystallization could be observed below 94 °C in the former case, the relative weakness of the precursor formation and lack of extended-chain crystal formation was apparent in the poor integrity of the fibers that were ultimately produced. Increasing the polymer concentration should lead to more effective entanglement and precursor formation; however, with our present apparatus flow experiments above 1 wt % were not possible due to the increased viscosity. Fortunately, the 1 wt % LMWPP solutions formed enough chain entanglements, without a dramatic increase in viscosity, so that the precursor formation mechanism could be directly observed.

Summary

By way of brief summary, these studies along with our earlier reports clearly substantiate that precursor formation followed by crystal growth is the fundamental process by which flow-induced crystallization occurs. The present studies also indicate the important role of polymer molecular weight and chain stiffness (whether inherent or induced by entanglement formation) in affecting both the rate and quality of the fibrillar precursor formation and subsequent oriented crystallization.

Acknowledgment. This work has been supported in part by research grants from 3M Co. and the National Science Foundation (Grant DMR 84-04968). We thank Himont U.S.A. Inc. and Shell Development Co. for supplying the polymers used in this study.

References and Notes

(1) Rietveld, J.; McHugh, A. J. *J. Polym. Sci., Polym. Phys. Ed.* **1983**, *21*, 1513.
(2) Pennings, A. J. *Proc. Int. Symp. Fiber Sci. Technol.*, Hakone, Japan, 1985; p 20.
(3) Rietveld, J.; McHugh, A. J. *J. Polym. Sci., Polym. Lett. Ed.* **1983**, *21*, 919.
(4) Rietveld, J.; McHugh, A. J. *J. Polym. Sci., Polym. Phys. Ed.* **1985**, *23*, 2339.
(5) McHugh, A. J.; Rietveld, J. *J. Polym. Sci., Polym. Phys. Ed.* **1985**, *23*, 2359.
(6) Vrahopoulou-Gilbert, E.; McHugh, A. J. *Macromolecules* **1984**, *17*, 2657.
(7) Vrahopoulou, E. P.; McHugh, A. J. *J. Appl. Polym. Sci.* **1986**, *31*, 399.
(8) Andruszka, K. W., personal communication.
(9) Vrahopoulou, E. P. Ph.D. Thesis, University of Illinois, Urbana, 1986.
(10) Graessley, W. W. *J. Chem. Phys.* **1965**, *43*, 15.
(11) Pelzbauer, Z.; Manley, R. St. John *J. Macromol. Sci., Phys.* **1970**, *B4*, 761.
(12) Blunk, R. H. M.S. Thesis, University of Illinois, Urbana, 1985.
(13) Pennings, A. J. *J. Polym. Sci., Part C* **1967**, *16*, 1799.
(14) McHugh, A. J. *Polym. Eng. Sci.* **1982**, *22*, 15.
(15) McHugh, A. J.; Ejike, E.; Silebi, C. A. *Polym. Eng. Sci.* **1979**,*19*, 414.
(16) Samuels, R. J. *Structured Polymer Properties*; Wiley: New York, 1974; Chapter 2.
(17) Shah, J. K.; Lahti, L. E. *Ind. Eng. Chem. Prod. Res. Dev.* **1973**, *12*, 304.
(18) Wikjord, A. G.; Manley, R. St. John *J. Macromol. Sci., Phys.* **1970**, *B4*, 397.
(19) Flanagan, R. D.; Rijke, A. M. *J. Polym. Sci., Part A-2* **1972**, *10*, 1207.
(20) Rijke, A. M.; McCoy, S. *J. Polym. Sci.* **1972**, *10*, 1845.

Laser Desorption–Fourier Transform Mass Spectrometry for the Characterization of Polymers

Robert S. Brown, David A. Weil, and Charles L. Wilkins*

Department of Chemistry, University of California—Riverside, Riverside, California 92521.
Received October 23, 1985

ABSTRACT: Laser desorption–Fourier transform mass spectrometry has been applied to a variety of polymers with average molecular weights of up to 6000. Spectra obtained are dominated by peaks corresponding to the K^+ or Na^+ attachment to the various oligomers, making molecular weight characterization simple. Calculated molecular weights for the polymers examined are in good agreement both with nominal values supplied by the manufacturers and with end-group titration values. No mass discrimination is observed in either the ionization mechanism or mass spectrometer up to masses of ~7000 amu, and no significant fragmentation is observed in the polymers studied.

The molecular weight distribution (MWD) of a polymer is an important factor in determining the suitability of a given polymer for a particular application. Other important parameters include chemical composition, stereochemistry, topology, and morphology. A variety of analytical techniques have been developed for characterizing the molecular weights of polymers. These can be divided into methods that provide average values of molecular weight and those that provide the full MWD. These can be subdivided further into absolute and relative methods,

0024-9297/86/2219-1255$01.50/0